

## The FLUKA code for space applications: recent developments

V. Andersen <sup>a</sup>, F. Ballarini <sup>b</sup>, G. Battistoni <sup>c</sup>, M. Campanella <sup>c</sup>, M. Carboni <sup>d</sup>,  
F. Cerutti <sup>c</sup>, A. Empl <sup>a</sup>, A. Fassò <sup>e,1</sup>, A. Ferrari <sup>e,c,\*</sup>, E. Gadioli <sup>c</sup>, M.V. Garzelli <sup>c</sup>,  
K. Lee <sup>a</sup>, A. Ottolenghi <sup>b</sup>, M. Pelliccioni <sup>d</sup>, L.S. Pinsky <sup>a</sup>, J. Ranft <sup>f</sup>, S. Roesler <sup>e</sup>,  
P.R. Sala <sup>g,c</sup>, T.L. Wilson <sup>h</sup>

<sup>a</sup> *Houston University, Texas, USA*

<sup>b</sup> *University of Pavia and INFN, Italy*

<sup>c</sup> *University of Milan and INFN, Via Celoria 16, 20133 Milan, Italy*

<sup>d</sup> *Laboratori Nazionali di Frascati, INFN, 00044 Frascati, Italy*

<sup>e</sup> *CERN, Geneva 23, CH-1211, Switzerland*

<sup>f</sup> *Siegen University, Germany*

<sup>g</sup> *ETH Zurich, Switzerland*

<sup>h</sup> *NASA/JSC, USA*

Received 15 October 2002; received in revised form 27 March 2003; accepted 30 March 2003

### Abstract

The FLUKA Monte Carlo transport code is widely used for fundamental research, radioprotection and dosimetry, hybrid nuclear energy system and cosmic ray calculations. The validity of its physical models has been benchmarked against a variety of experimental data over a wide range of energies, ranging from accelerator data to cosmic ray showers in the earth atmosphere. The code is presently undergoing several developments in order to better fit the needs of space applications. The generation of particle spectra according to up-to-date cosmic ray data as well as the effect of the solar and geomagnetic modulation have been implemented and already successfully applied to a variety of problems. The implementation of suitable models for heavy ion nuclear interactions has reached an operational stage. At medium/high energy FLUKA is using the DPMJET model. The major task of incorporating heavy ion interactions from a few GeV/n down to the threshold for inelastic collisions is also progressing and promising results have been obtained using a modified version of the RQMD-2.4 code. This interim solution is now fully operational, while waiting for the development of new models based on the FLUKA hadron–nucleus interaction code, a newly developed QMD code, and the implementation of the Boltzmann master equation theory for low energy ion interactions.

© 2004 COSPAR. Published by Elsevier Ltd. All rights reserved.

*Keywords:* FLUKA code; Space applications; Monte Carlo transport

### 1. Introduction

FLUKA (Fassò et al., 2001a,b) is a transport and interaction Monte Carlo code, capable of handling hadronic and electromagnetic showers from thermal neutrons up to very high energies (100 TeV). Being based, as far as possible, on well tested microscopic models, it ensures a high level of accuracy and versa-

tility, it preserves correlations within interactions and among the shower components, and it provides predictions where no experimental data is directly available. When needed, powerful biasing techniques are available to reduce computing time. Descriptions of FLUKA models and extensive benchmarking can be found in the literature (see the web page, [www.fluka.org](http://www.fluka.org)).

FLUKA is already widely used for cosmic ray related calculations. Two recent, important examples are the calculation of atmospheric neutrino fluxes (Battistoni et al., 2000), and the evaluation of aircraft exposure (Ferrari et al., 2001; Roesler et al., 2002). A vast amount of benchmarking with muon, hadron and electron data

\* Corresponding author. Tel.: +41-22-767-6119; fax: +41-22-767-7555.

E-mail address: [alfredo.ferrari@cern.ch](mailto:alfredo.ferrari@cern.ch) (A. Ferrari).

<sup>1</sup> Present address: SLAC, USA.

in atmosphere (Battistoni et al., 2002; Zuccon et al., 2001; Roesler et al., 2002) has confirmed that the accuracy of FLUKA hadronic interaction models makes it an ideal instrument in this field. A comparison of measured and computed muon fluxes in the atmosphere is shown in Fig. 1 as an example of the agreement with experimental data.

A modified version of FLUKA has also been specifically developed for radiobiological studies (with applications in radiation protection and radiotherapy) by including the results obtained with event-by-event Monte Carlo track structure codes (Biaggi et al., 1999, 2001) or including experimental data relative to particular radiobiological end-points (Ballarini et al., 2003). FLUKA is able to dynamically treat voxel geometries and has been coupled with mathematical and voxel anthropomorphic phantoms. It has been used to calculate physical and biological doses at the organs in different irradiation conditions (Ballarini et al., 2002, 2004).

Since ion–ion nuclear interactions were not yet treated in FLUKA, past results have been obtained in the superposition model, where primary nuclei were split into nucleons before interacting. With the integration of ion interaction codes and the cross-section parameterization as described below, this approximation is obsolete. Combined with further refinements in the treatment of primary cosmic spectra, solar modulations and the geomagnetic field, FLUKA now allows for an even higher simulation accuracy.

In the near future, new intermediate energy nucleus–nucleus generators will be developed to substitute the presently interfaced RQMD-2.4 code. In addition, the BME code developed at the University of Milan will be interfaced to cover the lowest energy ion–ion interactions.

## 2. The FLUKA–DPMJET interface

DPMJET-II.53 (Ranft, 1995), a Monte Carlo model for sampling hadron–hadron, hadron–nucleus and nucleus–nucleus collisions at accelerator and cosmic ray energies ( $E_{\text{lab}}$  from 5–10 GeV/n up to  $10^9$ – $10^{11}$  GeV/n), was adapted and interfaced to the FLUKA program. FLUKA implements DPMJET-II.53 as an event generator to simulate nucleus–nucleus interactions exclusively. DPMJET (as well as the FLUKA high energy hadron–nucleus generator) is based on the Dual Parton Model in connection with the Glauber formalism. The implementation of DPMJET is also considered a possible, future option to extend the FLUKA energy limits for hadronic simulations in general.

Internally, DPMJET uses Glauber impact parameter distributions per projectile–target combination. These are either computed during initialization of the program or can be processed and output in a dedicated run of DPMJET in advance. The computations are CPU intensive for colliding systems with heavier nuclei and it would not be practical to produce the required distributions repeatedly while processing full showers in FLUKA. Therefore, a procedure was devised to efficiently provide pre-computed impact parameter distributions for a complete matrix of projectile–target combinations up to a mass number of  $A = 246$  over the entire available energy range (Empl et al., 2002).

FLUKA requires AA reaction cross-sections internally in order to select nucleus–nucleus interactions appropriately. Hence, a complete matrix of AA reaction cross-sections was prepared along with the Glauber impact parameter distributions. Owing to the well established validity of the Glauber formalism, these cross-sections can be safely applied down to a projectile kinetic energy of  $\approx 1$  GeV/n.

DPMJET is called once per AA interaction. A list of final state particles as well as up to two excited residual nuclei with their relevant properties are returned by DPMJET for transport to FLUKA. De-excitation and evaporation of the excited residual nuclei is performed by calling the FLUKA evaporation module.

Work to interface DPMJET-3 (Roesler et al., 2001) is in progress. The upgrade is expected to be straightforward, in particular since the implemented scheme for both the pre-computed Glauber impact parameter distributions and the reaction cross-sections is compatible with DPMJET-3.

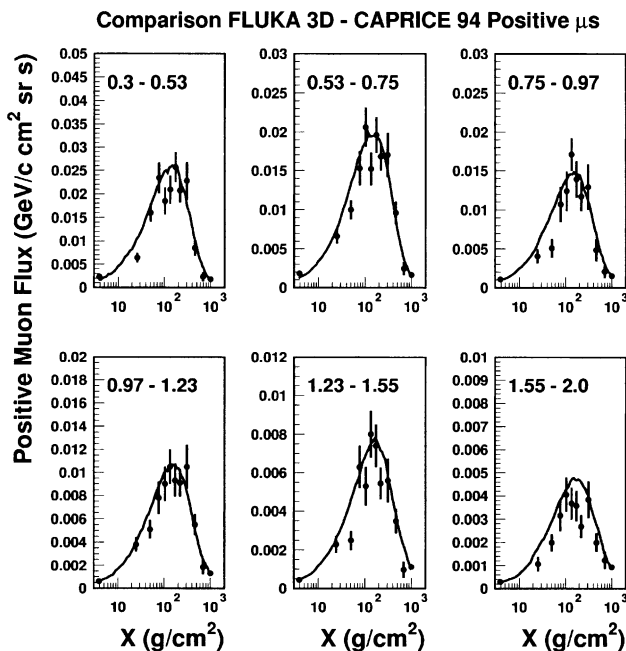


Fig. 1. Positive muon flux as a function of depth in the atmosphere, for various momentum intervals (GeV/c): symbols are experimental data, the line is the FLUKA simulation (adapted from Battistoni et al., 2002).

### 3. Low energy AA reaction cross-sections

To extend the range of AA reaction cross-section predictions for use in FLUKA down to the Coulomb barrier, a cross-section parameterization (Tripathi et al., 1999) was adopted. In general, this parameterization was found to work quite well at low energies. Discrepancies with respect to experimental data as well as to the DPMJET predictions were found however in case of the projectile kinetic energy approaching 1 GeV/n, depending on the combination of nuclear projectile and target. The origin of the discrepancies might partially be attributed to the available experimental data which historically we biased towards light systems with a large fraction of measurements at very low energies. In addition, early measurements of AA absorption (or production) cross-sections suffer from systematic uncertainties since they are model dependent.

The original model assumes the following form for the reaction cross-section:

$$\sigma_R = \pi r_o^2 \left( A_P^{1/3} + A_T^{1/3} + \delta_E \right)^2 \left( 1 - R_c \frac{B}{E_{cm}} \right) X_m,$$

with  $r_o = 1.1$  fm,  $A_P$  and  $A_T$  the projectile and target mass numbers, respectively, a Coulomb multiplier  $R_c$ , the energy dependent Coulomb barrier  $B$ , the kinetic energy in the center-of-momentum system  $E_{cm}$  and a further varying modifier  $X_m$  which only differs from unity for light systems.  $\delta_E$  is a rather complex expression depending on  $E$  which, besides others, includes the effects of Pauli blocking and transparency.

In order to address the found discrepancies, an *empirically* modified version of this parameterization was implemented in FLUKA. The modifications were derived using both experimental data and the DPMJET cross-section predictions at 3 GeV/n and applied to the com-

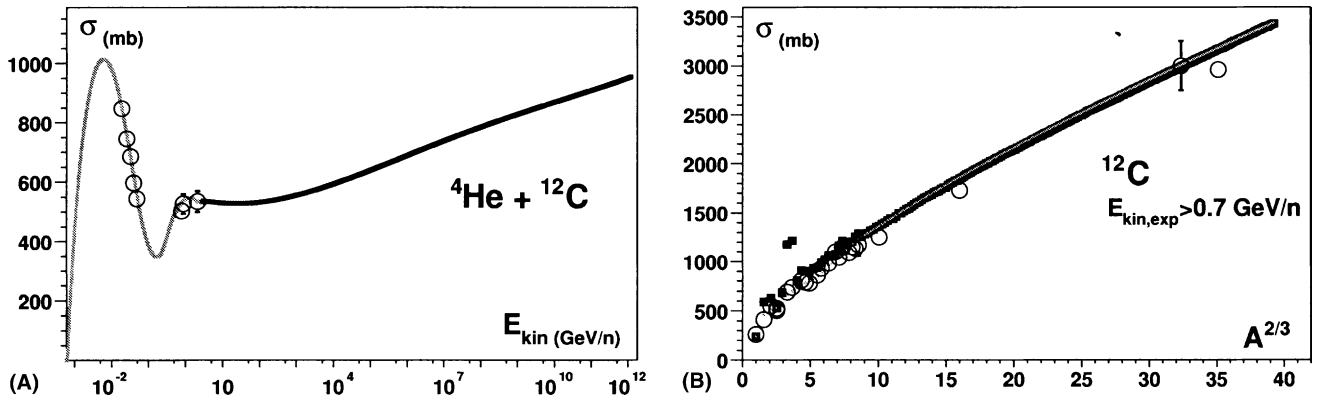


Fig. 2. (A) Combined reaction cross-section prediction for  ${}^4\text{He} + {}^{12}\text{C}$  as a function of kinetic energy given by the NASA parameterization (grey curve) and the DPMJET model (black curve). Open circles indicate the available experimental data. (B) Comparison of the NASA parameterization (solid black symbols) and the DPMJET reaction cross-section predictions (small grey symbols) at  $E_{kin} = 3$  GeV/n to available experimental data (open circles) for  ${}^{12}\text{C} + {}^A\text{X}$  as a function of  $A^{2/3}$ . Experimental results for projectile kinetic energies  $> 0.7$  GeV/n are included.

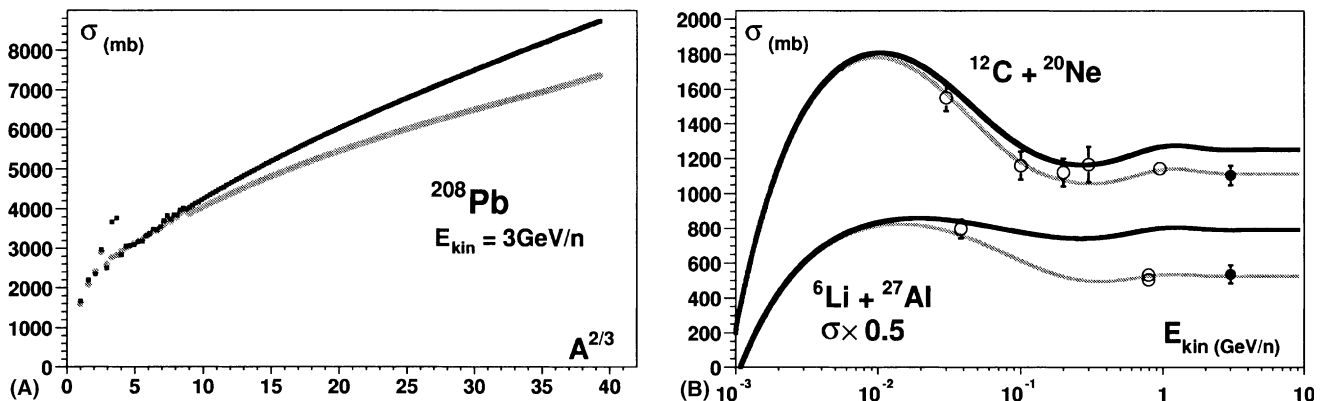


Fig. 3. (A) AA reaction cross-section predictions for  ${}^{208}\text{Pb}$  at  $E_{kin} = 3$  GeV/n as a function of  $A^{2/3}$ . The NASA parameterization (thin black curve) and the DPMJET model (grey curve) display a systematic discrepancy for heavy systems ( $A_P$  and  $A_T$  both greater than 26). The original parameterization was modified to smoothly join the DPMJET behavior close to projectile energies of  $E_{kin} \sim 1$  GeV/n. No experimental data is available for the systems at this energy. (B) Discrepancies for light systems: predictions of the original (thick black curves) and the modified (thin grey curves) NASA parameterization as a function of kinetic energy are compared to available data (open circles) for  ${}^{12}\text{C} + {}^{20}\text{Ne}$  (upper two curves) and  ${}^6\text{Li} + {}^{27}\text{Al}$  (lower two curves, scaled by 1/2). The solid black circles represent the DPMJET prediction for  $E_{kin} = 3$  GeV/n with an assumed 5% error.

putation of  $\delta_E$  only. Some additional work is required to finalize the implementation. The graphs in Fig. 2 demonstrate the quality of the original parameterization by comparison with experimental data and the DPMJET prediction for 3 GeV/n kinetic energy. In particular Fig. 2A displays the enormous range in energy for AA reaction cross-section now covered in FLUKA. The impact of the required modifications to the original parameterization is shown in Fig. 3 for a few selected cases. References for the experimental data are found in Tripathi et al. (1999) and references therein.

#### 4. The FLUKA–RQMD interface

Quantum-molecular-dynamics (QMD) approaches are a viable solution for nucleus–nucleus reactions. They represent an improvement over classical Intra Nuclear Cascade (INC) codes, thanks to their dynamic modeling of the nuclear field among nucleons during the reaction (more details about QMD can be found in the next two sections). The treatment of individual two-body scattering/interactions is usually based on similar approaches for INC and QMD codes. Unfortunately, initialization of the projectile and target nuclear states is often tricky and their relativistic extension somewhat problematic (see Section 5).

The RQMD-2.4 (Sorge et al., 1989; Sorge, 1995) is a relativistic QMD model which has been applied successfully to relativistic AA particle production over a wide energy range, from  $\approx 0.1$  GeV/n up to several hundreds of GeV/n. The high energy AA part in FLUKA is

already successfully covered by DPMJET. For energies below a few GeV/n several models are under development, either new, or based on the extension of the present intermediate energy hadron–nucleus model of FLUKA (see the next sections for more details). However, a RQMD-2.4 interface was developed meanwhile to enable FLUKA to treat ion interactions from  $\approx 100$  MeV/n up to 5 GeV/n where DPMJET starts to be applicable.

Several important issues had to be addressed. RQMD does not identify nuclei in the final state. Hence, no low energy de-excitation (evaporation, fragmentation, etc.) is performed for both the excited projectile and target residuals. This is highly problematic, particularly for the projectile residual, since its de-excitation usually gives rise to the highest energy particle production in the laboratory frame. Serious energy non-conservation issues are also affecting the code, particularly when run in full QMD mode (RQMD can run both in full QMD mode or in the so called “fast cascade” mode where it behaves similar to an INC code). Therefore a meaningful calculation of residual excitation energies was impossible.

The adopted solution was to modify the code, reworking the nuclear final state out of the available information on spectators, correlating the excitation energy to the actual hole depth of hit nucleons. Finally, the remaining energy–momentum conservation issues were resolved taking into account experimental binding energies, as is the case for all other FLUKA models. After these improvements a meaningful excitation energy could be computed and the FLUKA evaporation model was used to produce the low energy (in their respective

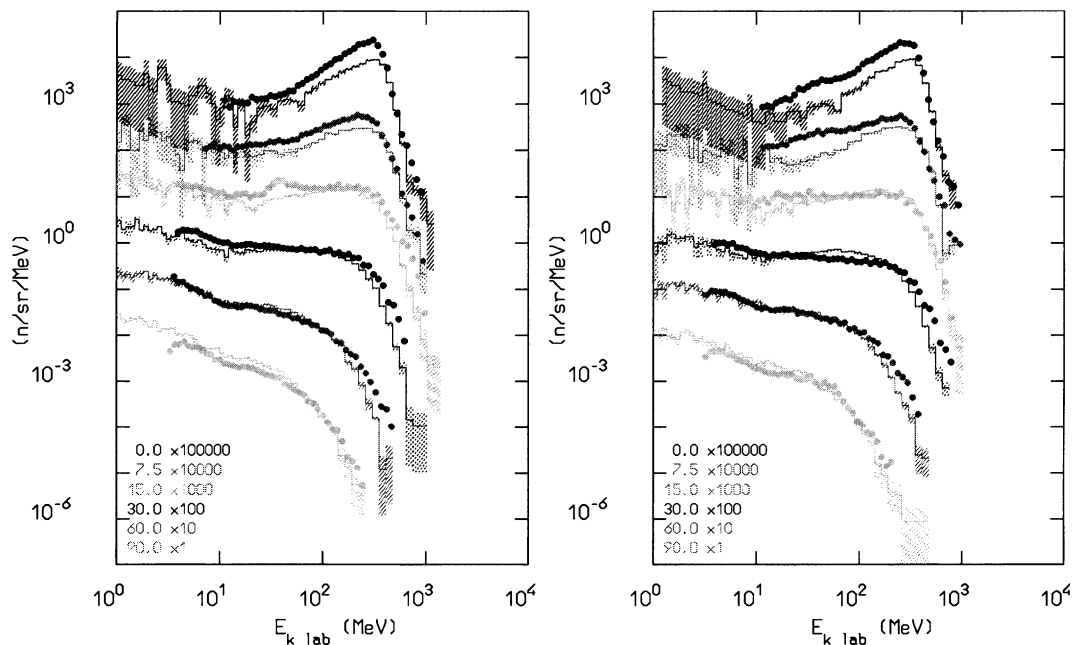


Fig. 4. Double differential neutron yield by 400 MeV/n Ar (left) and Fe (right) ions on thick Al targets. Data are shown for six different laboratory emission angles, with the most forward on top: histograms are FLUKA results, dots experimental data (Kurosawa et al., 2000).

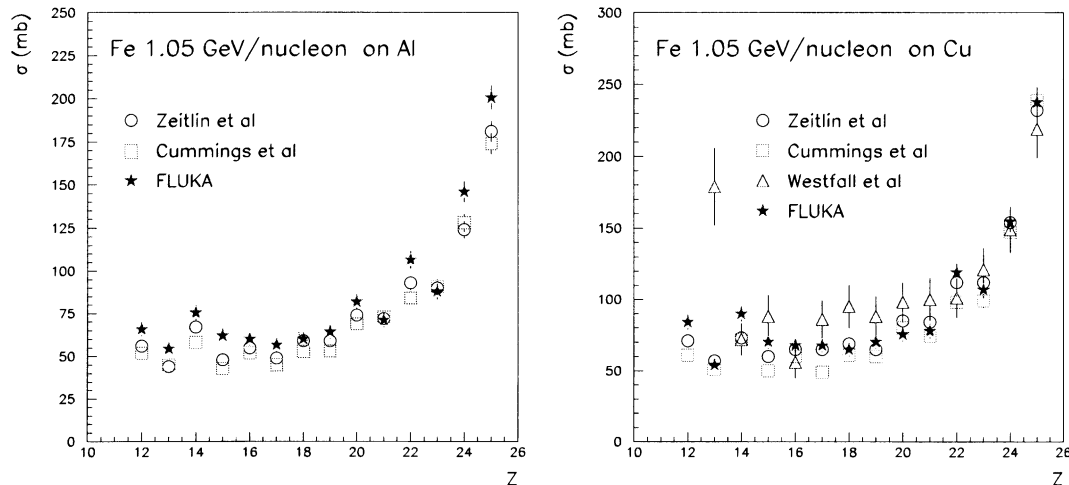


Fig. 5. Fragment charge cross-sections for 1.05 GeV/n Fe ions on Al (left) and Cu (right). Stars, FLUKA; circles, Zeitlin et al., 1997; squares, (1.5 GeV/n) Cummings et al., 1990; triangles, (1.88 GeV/n) Westfall et al., 1979.

rest frames) particles emitted by the excited projectile and target residuals.

Examples of the performances of FLUKA when running with the modified RQMD-2.4 model are presented in Figs. 4 and 5 and compared with experimental data, for double differential neutron production at 400 MeV/n and fragment production at 1.05 GeV/n, respectively. Despite these satisfactory results, the modified RQMD model is meant as a temporary solution for AA interactions below few GeV/n for FLUKA. Indeed the code is no longer developed or maintained and, given the shortcomings described before, in the long term we prefer to develop a new self-consistent QMD model where proper nuclear binding effects and excitation energy calculations are built in from the very beginning. While this solution, described in the next section, will cover the medium-heavy nuclei, the extension of the present FLUKA intermediate energy model to light ions (up to C), presently under testing, will provide a viable alternative for light ones.

## 5. QMD code development: an introduction to the model

QMD models were proposed by different groups in non-relativistic and relativistic form to simulate heavy-ion collisions at intermediate energies ( $30 \text{ MeV/n} \lesssim E \lesssim \text{a few GeV/n}$ ). From a microscopic point of view, a nuclear ground state is described as a set of nucleon configurations. Each nucleon is represented by a gaussian wave function and moves according to its Fermi kinetic energy inside the potential originating from all other nucleons. When two nuclei, evolving according to classical Hamiltonian equations of motion of their constituent nucleons, come close to each other, the nucleons feel the effect of a global potential which in-

fluences the collision process. Further, stochastic nucleon–nucleon scattering effects are introduced by Monte Carlo methods. Random sampling of the initial configuration for given  $A$  and  $Z$  is performed to select sets of initial spatial coordinates and momenta for the nucleon centroids, to reproduce as closely as possible the observed ground state properties.

The initialization process is one of the key difficulties in trying to implement a QMD model. Classically the minimum of the nuclear Hamiltonian provides a stable configuration in which all the nucleons freeze their Fermi motion and get into an overpopulated state where the Pauli principle is broken (Niita et al., 1995). Rather than choosing Hamiltonian minima as initial configurations of the QMD ground state, the selected configurations are forced to obey the Pauli principle. This choice however allows for spurious emission of individual nucleons and requires to ensure that the nuclear density profiles remain reasonably close to the experimental ones and that no spurious emission of nucleons occurs at least on the time scale of nuclear collision and fragment formation.

## 6. Light nuclear ground states from QMD Hamiltonian

QMD models simulate the total nuclear potential through two-nucleon and three-nucleon effective potentials. Several variants of these potentials can be found in the literature (see, for instance, Sorge et al., 1989; Aichelin, 1991; Niita et al., 1995; Souza et al., 1994; Wang et al., 2002; Papa et al., 2002). While interactions in field theory are local making easy the extension from a non-relativistic framework to a relativistic one, the problems in developing a relativistic program are due to the difficulty of implementing the

action at a distance in a covariant manner (Sorge et al., 1989). Thus, and because of the considered energy range, a non-relativistic framework was chosen, in particular following Wang et al., 2002.

Three nuclear potential terms are included: a *Skyrme* type potential with a two-body attractive and a three-body repulsive term, a *symmetry* term which takes into account the difference between proton and neutron densities, and a *surface* term, which is crucial for nuclear stability, preventing nucleons both from gathering in the nuclear center and escaping if close to the nuclear surface. The nuclear potential for the  $i$ th nucleon can be written as

$$V_i = \sum_{j,j \neq i} \left[ \frac{\alpha + |T_{zi} + T_{zj}| C_s}{2\rho_0} \int d\vec{r} \rho_i(\vec{r}) \rho_j(\vec{r}) \right. \\ \left. + \frac{g_{\text{tot}}}{2} \int \vec{\nabla} \rho_i(\vec{r}) \cdot \vec{\nabla} \rho_j(\vec{r}) d\vec{r} \right] \\ + \frac{\beta}{3\rho_0^2} \left[ \sum_{j,j \neq i} \int d\vec{r} \rho_i(\vec{r}) \rho_j(\vec{r}) \right]^2,$$

where  $\rho_i(\vec{r})$  is the nuclear density contribution at the point  $\vec{r}$  due to the  $i$ th nucleon, and  $T_{zi}$  its isospin component. In addition, a repulsive *Coulomb* term between protons is introduced that cannot be neglected at non-relativistic energies. It should be emphasized that the compensation between attraction and repulsion is crucial for nuclear stability. It follows that the stability is sensitive not only to the functional form of the potential terms, but also to the values of the potential parameters involved in these terms. The following values were adopted for the potential parameters in this work:  $\alpha = -124$  MeV,  $\beta = 71$  MeV,  $C_s = 32$  MeV,  $g_{\text{tot}} = 550$  MeV fm<sup>5</sup>, where the first two parameters appear in the expression of the Skyrme-type potential terms,  $C_s$  is the symmetry term coefficient, and  $g_{\text{tot}}$  is related to the surface term. For this choice of parameters, more than

half of the “random” initial configurations produce “stable” conditions for light nuclei ( $8 \leq A \leq 24$ ), i.e., they do not give rise to spurious nucleon emission at least within 200 fm/c, as can be seen in case of <sup>16</sup>O nuclei in Fig. 6 (left). The initialization procedure automatically generates rms radii close to those obtained with the empirical formula  $\sqrt{\langle R_A^2 \rangle} = 0.82A^{1/3} + 0.58$  fm which then vary depending on the Hamiltonian during the time evolution. Only configurations which do not produce spurious emission of nucleons are considered for subsequent nucleus–nucleus collision simulations. Further checks on energy conservation and the time evolution of the spatial and momentum density distributions were performed. Indeed, it was found that the spatial density profile does not change much from the initial distribution during propagation (see Fig. 6, right), while the momentum distribution is more affected.

With regards to the momentum distributions, it is noted that the initial distributions tend to evolve to classical ones with a great number of nucleons with very low momenta and few nucleons with higher momenta. This effect is in part responsible for the lack of stability and is more evident for heavier nuclei. Tentative solutions are proposed in literature in order to reduce this trend. Constraints proposed by Papa et al. (2002) are currently under investigation to assess in particular their effectiveness in improving the stability of nuclei heavier than those considered in this work ( $A \gtrsim 30$ ). More details on the described initialization procedures will be published soon in a separate paper.

## 7. The BME model

The Boltzmann master equation (BME) theory, which is especially useful for describing heavy ion reactions, predicts the time evolution of the momentum distribution of the nucleons of an excited nucleus

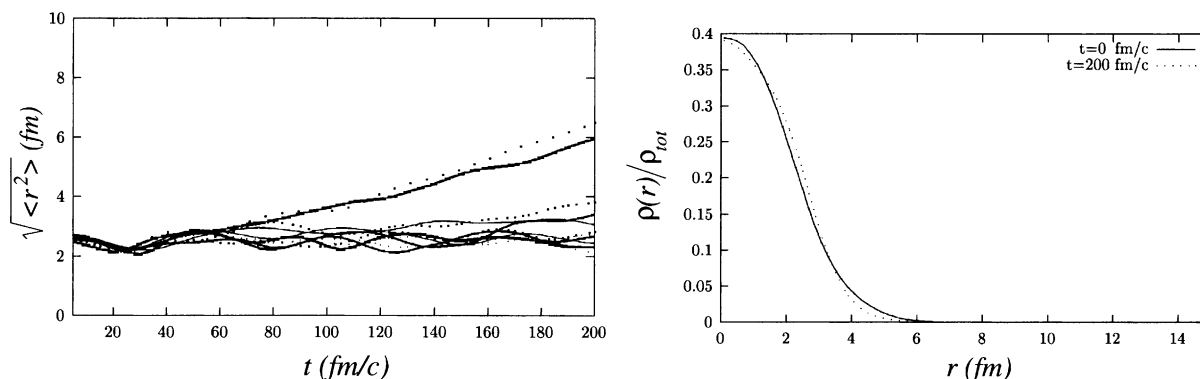


Fig. 6. (left) Root mean square radii of <sup>16</sup>O nuclei (fm) versus time (fm/c) for eleven initial random configurations obtained using the potentials and the potential parameter values indicated above. About 1/2 of them can be stored as “stable” configurations. (right) Normalized spatial density distribution as a function of radius, at the beginning of the time evolution (solid line) and after 200 fm/c (dotted line), of the most “stable” <sup>16</sup>O nuclear configuration among those shown on the left.

created in the interaction of two ions. To do that, the nucleon's momentum space is binned and the variation with time of the occupation probability of the states of each bin is evaluated as a result of nucleon–nucleon interactions and the emission into the continuum of single nucleons and nucleons bound in clusters. Assuming azimuthal symmetry with respect to the beam direction, with a simple change of variables, the occupation probability  $n_i$  of the states of a given bin  $i$  may be estimated as a function  $n_i(\epsilon, \theta, t)$  of the nucleon energy  $\epsilon$ , its direction  $\theta$  with respect to the beam, and the time  $t$ . It may be calculated by integrating a set of coupled equations which express its variation in a small time interval between  $t$  and  $t + dt$  as a function of the occupation probabilities at time  $t$  and the probabilities per time unit (decay rates) of occurrence of the processes indicated above. This procedure allows one to evaluate also the double differential spectra of the particles which are emitted in the considered time interval, and, by integrating over time, the spectra of particles emitted in the reaction. To integrate the BMEs one must know the bin's occupation probabilities at an initial time  $t = 0$ , which depend on the dynamics of the two ion interaction. The theory is expounded in a series of papers in which the expressions of the decay rates of the various processes which may occur are given and its predictions are compared to a large set of experimental data (Fabrici et al., 1989; Cervesato et al., 1992; Cavinato et al., 1994; Brusati et al., 1995; Cavinato et al., 1998). For present purposes, it may be useful to briefly discuss how the results of the integration of the BMEs may be used as an input for Monte Carlo calculations which allow to evaluate the probability of particular sequences of events such as those observed in an exclusive experiment or those which lead to the formation of a particular

residue in a reaction. This probability cannot be estimated simply by solving the set of BMEs which may only give results averaged over many reaction paths. It has also to be stressed that, in the theory, the natural reference frame is the Centre of Mass of the two interacting ions which is assumed to have an infinitely large mass so, in those cases where the nuclear recoils during a sequence of particle emissions have to be taken into account, the theoretical calculations cannot reproduce exactly even the results of an inclusive experiment which are referred to the Laboratory System. To solve this problem the differential multiplicity  $d^3M(\epsilon, \theta, t)$  of a given particle can be assumed as the probability of emitting that particle with energy  $\epsilon$  and direction  $\theta$  in the time interval between  $t$  and  $t + dt$ . From these *elementary* probabilities one may evaluate the probability of any pre-determined complex event as a joint probability, according to the method discussed in Cavinato et al. (1996, 2001) which allows to perform, for each emission, the proper transformation from the Center of Mass of the decaying nucleus to the Laboratory System.

In this paper we cannot discuss further the outlined theory and we limit ourselves to show three examples of the results which may be obtained. Fig. 7 compares experimental data on neutron production with the results of the detailed simulation of the experiment (Cavinato et al., 2001). Fig. 8 shows the spectra of carbon fragments emitted in the interaction of 400 MeV  $^{16}\text{O}$  ions with  $^{59}\text{Co}$  at  $4^\circ$ ,  $24^\circ$  and  $50^\circ$ . At  $4^\circ$  the spectra are dominated by fragments produced in the binary fragmentation of oxygen. At larger angles the contribution of low energy fragments produced by nucleon coalescence during the series of nucleon–nucleon interactions described by the BMEs becomes progressively dominant. Histograms and full lines represent the two

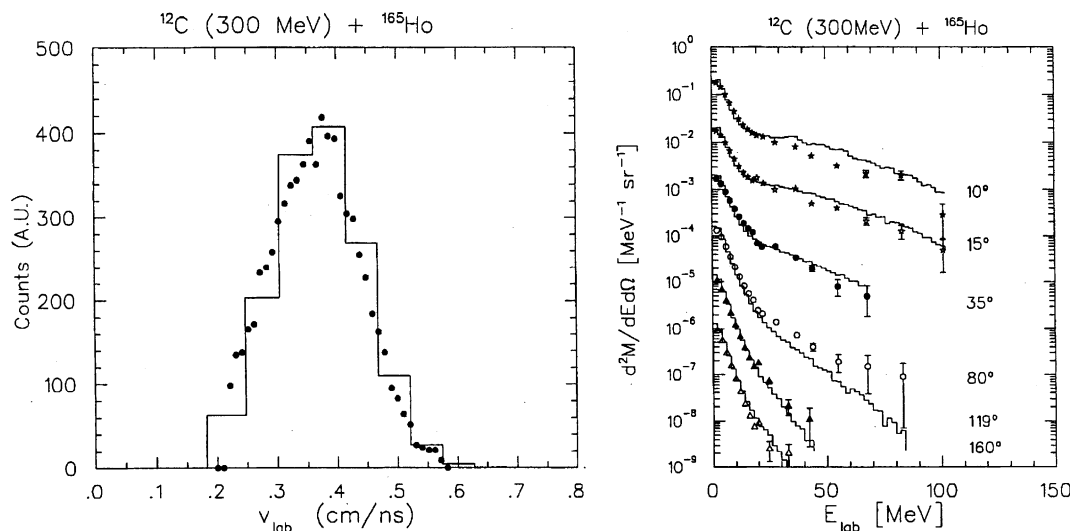


Fig. 7. On the right, double differential spectra of neutrons emitted in  $^{12}\text{C} + ^{165}\text{Ho}$  at 25 MeV/n in coincidence with evaporation residues emitted at  $7.5 \pm 1.2^\circ$ , whose velocity distribution is shown on the left (Holub et al., 1986). Dots are experimental data, histograms are simulation results.

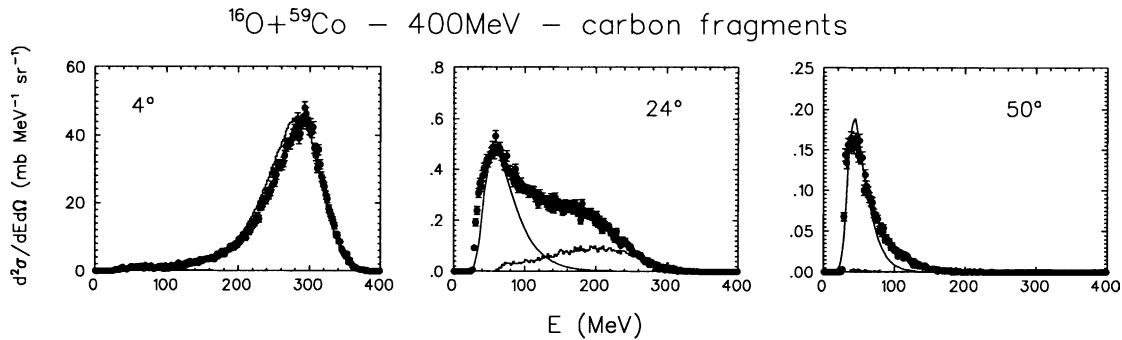


Fig. 8. Experimental (symbols) and calculated (lines) spectra of carbon fragments emitted in the interaction of 400 MeV  $^{16}\text{O}$  ions with  $^{59}\text{Co}$  at different angles (see text).

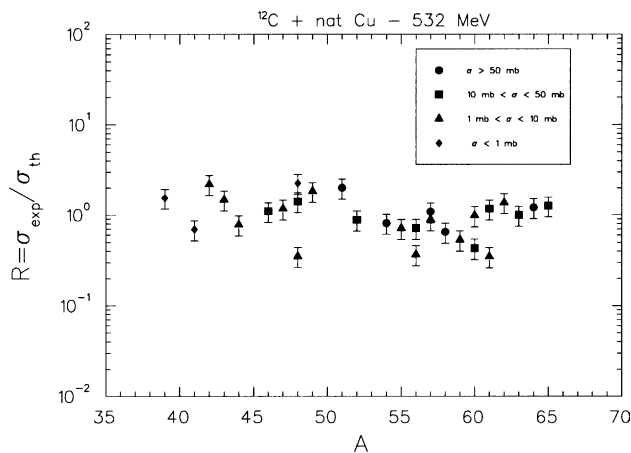


Fig. 9. Ratio between measured and calculated cross-sections for residue formation, as a function of the residue mass, in the interaction of 45 MeV/n  $^{12}\text{C}$  with natural copper.

contributions (from binary fragmentation and nucleon coalescence, respectively) as predicted by the theory, reproducing satisfactorily the measured spectrum (Gadioli et al., 2002). Fig. 9 shows the ratio between the measured and the calculated cross-sections for residue formation in the interaction of 45 MeV/n  $^{12}\text{C}$  ions with natural copper. Most of experimental cross-sections are reproduced within a factor of two and often with much better accuracy. What is even more encouraging is the fact that the accuracy in reproducing the data is independent on the cross-section value which varies by more than two orders of magnitude (Cho et al., 1989). So far the BME theory has been used for incident energies up to 50 MeV/n. We intend to extend its predictions up to about 100 MeV/n.

## 8. Conclusions

The FLUKA Monte Carlo code is used in many fields, from basic research to radiation protection and dosimetry, radiobiology, and energy production. In particular,

FLUKA is already a widespread and reliable tool for cosmic ray shower simulations. Besides the basic transport and interaction parts, also the other ingredients of the simulations, from primary spectra to geomagnetic fields, have been carefully modeled. The recent addition of interfaces to ion–ion interaction codes allows to better simulate the heavy ion component of the cosmic radiation. The results are very encouraging and demonstrate that the code can already be applied to practical problems. However, further improvements of the nucleus–nucleus intermediate energy modeling are planned. First steps towards the development of a dedicated QMD model have been taken, demonstrating the feasibility of the project. Work is in progress to cover also the lowest energy range (below 100 MeV/n) through a Monte Carlo Boltzmann master equation code and its concepts and performances have been briefly illustrated.

## Acknowledgements

This work was partially supported under NASA Grant NAG8-1658, ASI contract 1/R/320/02, and EC contract FIGH-CT1999-00005.

## References

- Aichelin, J. QMD-A dynamical microscopic N-body approach to investigate fragment formation and the nuclear EOS in heavy ion collisions. *Phys. Rep.* 202, 233–360, 1991.
- Ballarini, F., Biaggi, M., Edwards, A., et al. Estimating mixed field effects: an application supporting the lack of a non-linear component for chromosome aberration induction by neutrons. *Radiat. Prot. Dosim.* 103, 19–27, 2003.
- Ballarini, F., Biaggi, M., Ferrari, A., et al. Modelling the influence of shielding on physical and biological organ doses. *J. Radiat. Res.* 43, 99–102, 2002.
- Ballarini, F., Biaggi, M., De Biaggi, L., et al. Role of shielding in modulating the effects of Solar Particle Events: Monte Carlo calculation of physical and biological dose in different organs. *Adv. Space Res.*, this issue, 2004, doi:10.1016/j.asr.08.055.

- Battistoni, G., Ferrari, A., Lipari, P., Montaruli, T., Sala, P.R., Rancati, T. A 3-dimensional calculation of the atmospheric neutrino fluxes. *Astropart. Phys.* 12, 315–333, 2000.
- Battistoni, G., Ferrari, A., Montaruli, T., Sala, P.R. Comparison of the FLUKA calculations with CAPRICE 94 data on muons in atmosphere. *Astropart. Phys.* 17, 477–488, 2002.
- Biaggi, M., Ballarini, F., Burkard, W., et al. Physical and biophysical characteristics of a fully modulated 72 MeV therapeutic proton beam: model predictions and experimental data. *Nucl. Instr. Meth. B* 159, 89–100, 1999.
- Biaggi, M., Ballarini, F., Ferrari, A., et al. A Monte Carlo code for a direct estimation of radiation risk. *Phys. Med.* 17/S1, 103–105, 2001.
- Brusati, C., Cavinato, M., Fabrici, E., et al. Nuclear surface, mean field and isospin effects in Boltzmann master equation theory of pre-equilibrium reactions. *Z. Phys. A* 353, 57–69, 1995.
- Cavinato, M., Fabrici, E., Gadioli, E., Gadioli Erba, E., Galbiati, E. Monte Carlo calculations using the Boltzmann master equation theory of nuclear reactions. *Phys. Lett. B* 382, 1–5, 1996.
- Cavinato, M., Fabrici, E., Gadioli, E., Gadioli Erba, E., Risi, E. Boltzmann master equation theory of angular distributions in heavy-ion reactions. *Nucl. Phys. A* 643, 15–29, 1998.
- Cavinato, M., Fabrici, E., Gadioli, E., Gadioli Erba, E., Riva, G. Monte Carlo calculations of heavy ion cross-sections based on the Boltzmann master equation theory. *Nucl. Phys. A* 679, 753–764, 2001.
- Cavinato, M., Fabrici, E., Gadioli, E., et al. Intermediate mass fragment emission in Boltzmann master equation theory of pre-equilibrium reactions. *Z. Phys. A* 347, 237–245, 1994.
- Cervesato, I., Fabrici, E., Gadioli, E., Gadioli Erba, E., Galmarini, M. Light particle emission in Boltzmann master equation theory of pre-equilibrium reactions. *Phys. Rev. C* 45, 2369–2378, 1992.
- Cho, S.Y., Porile, N.T., Morrissey, D.J. Target residues from the interaction of copper with 15–45 MeV/nucleon  $^{12}\text{C}$  ions. *Phys. Rev. C* 39, 2227–2236, 1989.
- Cummings, J.R., Binns, W.R., Garrard, T.L., et al. Determination of the cross-sections for the production of fragments from relativistic nucleus–nucleus interactions. I. Measurements. *Phys. Rev. C* 42, 2508–2529, 1990.
- Empl, A., Fassò, A., Ferrari, A. et al. Progress and applications of FLUKA, in: Proceedings of the ANS Radiation Protection & Shielding Division 12th Topical Meeting, Santa Fe, New Mexico, USA, April 14–18, 2002 (6 p, published in electronic format).
- Fabrici, E., Gadioli, E., Gadioli Erba, E., et al. Importance of nucleon–nucleon interactions in hardening nucleon spectra in heavy ion fusion. *Phys. Rev. C* 40, 2548–2557, 1989.
- Fassò, A., Ferrari, A., Ranft, J., Sala, P.R. FLUKA: status and prospective for hadronic applications, in: Proceedings of the MonteCarlo 2000 Conference, Lisbon, October 23–26, 2000. Springer-Verlag, Berlin, pp. 955–960, 2001.
- Fassò, A., Ferrari, A., Sala, P.R. Electron–photon transport in FLUKA: status, in: Proceedings of the MonteCarlo 2000 Conference, Lisbon, October 23–26, 2000. Springer-Verlag, Berlin, pp. 159–164, 2001.
- Ferrari, A., Pelliccioni, M., Rancati, T. Calculation of the radiation environment caused by galactic cosmic rays for determining air crew exposure. *Rad. Prot. Dosim.* 93, 101–114, 2001.
- Gadioli, E., Steyn, G.F., Birattari, C., et al. Interplay of mean field and nucleon–nucleon interactions in the production of carbon fragments in  $^{16}\text{O}$  induced reactions at incident energies up to 25 MeV/amu. *Nucl. Phys. A* 708, 391–412, 2002.
- Holub, E., Hilscher, D., Ingold, G., et al. Preequilibrium neutron emission in fusion of  $^{165}\text{Ho} + ^{12}\text{C}$  at 25 MeV per nucleon. *Phys. Rev. C* 33, 143–152, 1986.
- Kurosawa, T., Nakao, N., Nakamura, T., et al. Neutron yields from thick C, Al, Cu and Pb targets bombarded by 400 MeV/nucleon Ar, Fe, Xe and 800 MeV/nucleon Si ions. *Phys. Rev. C* 62, 044615-1, 11.
- Niita, K., Chiba, S., Maruyama, T., et al. Analysis of the  $(\text{N}, \text{xN}')$  reactions by quantum molecular dynamics plus statistical decay model. *Phys. Rev. C* 52, 2620–2635, 1995.
- Papa, M., Maruyama, T., Bonasera, A. Constrained molecular dynamics approach to fermionic systems. *Phys. Rev. C* 64, 024612-1, 6.
- Ranft, J. Dual Parton Model at cosmic ray energies. *Phys. Rev. D* 51, 64–84, 1995.
- Roesler, S., Engel, R., Ranft, J. The Monte Carlo event generator DPMJET III, in: Proceedings of the MonteCarlo 2000 Conference, Lisbon, October 23–26, 2000. Springer-Verlag, Berlin, pp. 1033–1038, 2001.
- Roesler, S., Heinrich, W., Schraube, H. Monte Carlo calculation of the radiation field at aircraft altitudes. *Rad. Prot. Dosim.* 98, 367–388, 2002.
- Sorge, H. Flavor production in Pb (160 A GeV) on Pb collision: effect of color ropes and hadronic rescattering. *Phys. Rev. C* 52, 3291–3314, 1995.
- Sorge, H., Stocker, H., Greiner, W. Poincaré invariant hamiltonian dynamics: modelling multi-hadronic interactions in a phase space approach. *Ann. Phys.* 192, 266–306, 1989.
- Souza, S.R., de Paula, L., Leray, S., et al. A dynamical model for multifragmentation of nuclei. *Nucl. Phys. A* 571, 159–184, 1994.
- Tripathi, R.K., Cucinotta, F.A., Wilson, J.W. Accurate universal parameterization of absorption cross-sections III – light systems. *Nucl. Instr. Meth. B* 155, 349–356, 1999.
- Wang, N., Li, Z., Wu, X. Improved quantum molecular dynamics model and its applications to fusion reaction near barrier. *Phys. Rev. C* 65, 2002, 064608-1, 10.
- Westfall, G.D., Wilson, L.W., Lindstrom, P.J., et al. Fragmentation of relativistic  $^{56}\text{Fe}$ . *Phys. Rev. C* 19, 1309–1323, 1979.
- Zeitlin, C., Heilbronn, L., Miller, J., et al. Heavy fragment production cross-sections from 1.05 GeV/nucleon  $^{56}\text{Fe}$  in C, Al, Cu, Pb and  $\text{CH}_2$  targets. *Phys. Rev. C* 56, 388–397, 1997.
- Zuccon, P., Bertucci, B., Alpat, B., et al. A MonteCarlo simulation of the interaction of cosmic rays with the atmosphere, Report CERN-OPEN-2001-068, 2001.